Int. J. Corros. Scale Inhib., 2024, **13**, no. 3, 1590–1606

1590

The influence of the chemical structure of 3-mercapto- and 3-sulfinyl derivatives of 5-amino-1*H*-1,2,4-triazoles on their inhibitory ability against chloride-induced copper corrosion

A.A. Kruzhilin, D.S. Shevtsov, A.Yu. Potapov, M.Yu. Krysin and Kh.S. Shikhaliev*

Voronezh State University, 1 Universitetskaya pl., 394018 Voronezh, Russian Federation
*E-mail: shikh1961@yandex.ru

Abstract

The aim of this study is to investigate the anticorrosive properties of 5-amino-1*H*-1,2,4-triazole derivatives by introducing substituents such as thioacetonitrile and thioacetic acid fragments, as well as their mild oxidation products – sulfinylacetonitrile and sulfinylacetic acid. The synthesis methodology involved a sequence of two transformations: alkylation of 3-mercapto-5-amino-1*H*-1,2,4-triazole with chloroacetonitrile or monochloroacetic acid followed by the oxidation of the resulting 3-(alkylthio)-5-amino-1*H*-1,2,4-triazoles. The synthesized inhibitors were identified using high-performance liquid chromatography with high-resolution mass spectrometry detection (HPLC-HRMS-ESI) and UV detection, as well as NMR spectroscopy. Gravimetric and polarization corrosion tests were conducted on M1 copper samples in 1% chloride solutions. The highest inhibitory activity was exhibited by 2-((5-amino-1*H*-1,2,4-triazol-3-yl)sulfinyl)acetonitrile **3a** at a concentration of 0.10 mmol·dm^{-3}, providing significant protection without compromising the solubility of the inhibitor in aqueous solutions. The results of the study indicate that the introduction of an acetonitrile fragment into the chemical structure of 1,2,4-triazole-class inhibitors leads to a significant increase in their inhibitory efficiency against copper corrosion. Moreover, the application of sulfoxides based on the investigated alkylthiotriazoles results in an additional increase in the protective properties of these compounds, which is most pronounced for 2-((5-amino-1*H*-1,2,4-triazol-3-yl)sulfinyl)-acetonitrile.

1. Introduction

Copper and its alloys have found extensive applications in various industries due to their high thermal and electrical conductivity, ease of mechanical processing, and ease of soldering. Additionally, copper possesses specific qualities, such as preventing fouling of equipment used in marine environments by various microscopic organisms, since its ions are detrimental to algae and mollusks [1]. This makes it useful in shipbuilding, fisheries, and

similar fields. However, like most metals, copper suffers from corrosion, especially localized forms such as pitting corrosion, which primarily occurs upon contact with aggressive liquid environments like chlorides. One of the most common methods to reduce the rate of degradation under various conditions is the use of special organic corrosion inhibitors [2]. Heterocyclic compounds from the azole class are among the most frequently used commercial organic copper corrosion inhibitors [3, 4]. Many of these compounds have a range of beneficial properties, such as good water solubility, high thermal stability, environmental friendliness, cost-effectiveness, antimicrobial, and bactericidal activities, among others [5, 6]. The inhibitory properties of azoles [7–11] are due to the fact that hydrogen atoms directly bonded to nitrogen in the azole ring are highly mobile, making these structures N–H acids. As a result, there is a possibility for the inhibitor molecule to interact with the metal surface, adsorb on it, and form protective films [12] through ligand-acceptor complexation.

Despite the many known compounds with proven inhibitory effects, there is still a need to study new properties of corrosion inhibitors for specific metals under particular conditions, as well as for universal substances applicable to various metals and alloys used in diverse environments [13, 14]. The most studied corrosion protection agent for copper in the azole class is 1,2,3-benzotriazole [15–17], which is widely used to protect non-ferrous metals today. However, besides benzotriazole derivatives, some other more hydrophilic triazoles also attract researchers' attention for protecting copper and its alloys [18–20]. For example, 3-amino-1,2,4-triazole is found to be more effective than benzotriazole in preventing pitting on copper in a borate buffer solution containing chlorides or sulfates [21].

At the same time, one of the structure-oriented methods to increase the inhibitory efficiency of 3-amino-1,2,4-triazoles is the introduction of a hydrophobic substituent into the triazole ring [22]. However, this reduces their water solubility and can lead to equipment malfunction, including clogging of conductive channels with particle agglomerates [23]. Therefore, creating corrosion inhibitors with high protective ability and sufficient solubility is an important scientific and practical task.

The present article is a logical continuation of the authors' previous publications dedicated to the directed synthesis and investigation of the anticorrosion properties of 5-amino-1*H*-1,2,4-triazole derivatives in copper corrosion [24–27]. Its primary objective is to determine the influence of introducing electron-acceptor substituents such as thioacetonitrile and thioacetic acid, as well as their mild oxidation products – sulfinylacetonitrile and sulfinylacetic acid – into the structure of 5-amino-1*H*-1,2,4-triazoles on their protective properties against copper corrosion in 1% chloride-containing solutions.

2. Experimental

2.1. Methods of analyzing the chemical structure and composition of inhibitors

To analyze and confirm the structure of the synthesized inhibitors, high-performance liquid chromatography with high-resolution mass spectrometry detection at electrospray ionization

(HPLC-HRMS-ESI) combined with UV detection was used. The setup consisted of an Agilent 1269 Infinity liquid chromatograph and an Agilent 6230 TOF LC/MS high-resolution time-of-flight mass detector. Quantitative determination was performed using the internal standard method. ^{1}H NMR spectra were recorded on a Bruker AV600 spectrometer (600.13 MHz) in DMSO-d6, with TMS as the internal standard.

2.2. Synthesis and analysis of inhibitors

In line with the research objective, we synthesized new derivatives of 3-(alkylthio)-5-amino-1*H*-1,2,4-triazoles containing nitrile and acetic acid fragments, as well as the corresponding sulfoxide groups. The synthesis methodology involved a sequence of two transformations: alkylation of 3-mercapto-5-amino-1*H*-1,2,4-triazole with chloroacetonitrile or monochloroacetic acid followed by oxidation of the resulting 3-(alkylthio)-5-amino-1*H*-1,2,4-triazoles. The alkylation process was conducted using a previously optimized method [28] with ethanol as the solvent. The sodium salt was generated by reacting sodium hydroxide with mercaptan **1** under brief heating and stirring in ethanol. Alkylating agents, chloroacetonitrile and chloroacetic acid, were introduced into the reaction using a slight 10% molar excess.

R= NCCH$_2$ **(a);** HOOCCH$_2$ **(b)**
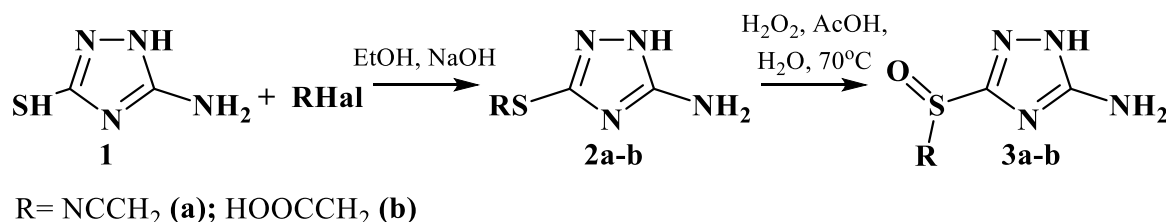
One of the promising methods for synthesizing sulfoxides and sulfones is the oxidation of organic sulfides with peroxides [29]. In this study, we found that oxidation of the synthesized 3-*R*-mercapto-5-aminotriazoles **2a–b** with hydrogen peroxide in the presence of an equimolar amount of acetic acid results in the formation of new 3-(*R*-sulfinyl)-5-amino-1,2,3-triazoles **3a–b**. The best conditions for the process involved adding hydrogen peroxide to a mixture of the starting mercaptotriazole, acetic acid, and water heated to 70°C. Complete oxidation of the substrate required a 1.5-fold amount of H$_2$O$_2$. As a result, 3-(*R*-mercapto)aminotriazoles **2a–b** and 3-(*R*-sulfinyl)aminotriazoles **3a–b** were synthesized with high preparative yields, and their chemical structures are presented in Table 1.

Table 1. List of investigated inhibitors.

Symbol	Name	Formula
2a	2-((5-Amino-1*H*-1,2,4-triazol-3-yl)thio)acetonitrile	

Symbol	Name	Formula
2b	2-((5-Amino-1*H*-1,2,4-triazol-3-yl)thio)acetic acid	
3a	2-((5-Amino-1*H*-1,2,4-triazol-3-yl)sulfinyl)acetonitrile	
3b	2-((5-Amino-1*H*-1,2,4-triazol-3-yl)sulfinyl)acetic acid	

*General procedure for the synthesis of 3-(R-mercapto)-5-amino-1H-1,2,4-triazoles **2a−b***

In a round-bottom flask, 0.1 mol of 3-mercapto-5-amino-1*H*-1,2,4-triazole **1** and 5.3 g of sodium hydroxide were dissolved in 30 ml of ethanol with stirring. Subsequently, 0.11 mol of the corresponding alkyl halide was added dropwise to the resulting mixture under vigorous stirring. The mixture was stirred and heated for 1–2 hours, depending on the reactivity of the alkylating agent. After evaporating the ethanol, the residue was triturated with 20 ml of water, the reaction product was filtered, washed with water, and dried at 60°C.

*2-((5-amino-1H-1,2,4-triazol-3-yl)mercapto)acetonitrile **2a***

Yield 54–56%, m.p. 136–138°C. White powder. ^{1}H NMR spectrum: 4.36 (s, 2H, CH$_2$), 6.82 (s, 2H, NH$_2$), 12.30 (s, 1H, NH). Found, *m/z*: 156.0339 [M+H]$^+$. C$_4$H$_5$N$_5$S+H$^+$. Calculated, *m/z*: 156.0339 [M+H]$^+$.

*2-((5-amino-1H-1,2,4-triazol-3-yl)mercapto)acetic acid **2b***

Yield 67–69%, m.p. 123–125°C. White powder. ^{1}H NMR spectrum: 4.30 (s, 2H, CH$_2$, *J* 14.3), 6.96 (s, 2H, NH$_2$), 11.24 (br.s., 1H, COOH); 12.61 (s, 1H, NH). Found, *m/z*: 175.0234 [M+H]$^+$. C$_4$H$_6$N$_4$O$_2$S+H$^+$. Calculated, *m/z*: 175.0211 [M+H]$^+$.

*General procedure for the synthesis of 3-(R-sulfinyl)-5-amino-1H-1,2,4-triazoles **3a−b***

A solution of 0.1 mol of the corresponding 3-(*R*-mercapto)-5-amino-1*H*-1,2,4-triazole **2a−b** and 6 ml of acetic acid in 150 ml of distilled water was heated to 70°C, and 15 g (0.15 mol) of hydrogen peroxide was added dropwise over 30 minutes. The mixture was kept at this temperature for another 2.5 hours and then cooled to 10°C. The precipitated reaction product was filtered, washed with 20 ml of cold water, and recrystallized from isopropanol after drying.

*2-((5-amino-1H-1,2,4-triazol-3-yl)sulfinyl)acetonitrile **3a***

Yield 68–70%, m.p. 195–197°C. White powder. ^{1}H NMR spectrum: 4.45 (d, 2H, CH$_2$, *J* 15.8), 4.57 (d, 2H, CH$_2$, *J* 15.8), 6.56 (s, 2H, NH$_2$), 12.87 (s, 1H, NH). Found, *m/z*: 172.0295 [M+H]$^+$. C$_4$H$_5$N$_5$OS+H$^+$. Calculated, *m/z*: 172.0288 [M+H]$^+$.

*2-((5-amino-1H-1,2,4-triazol-3-yl)sulfinyl)acetic acid **3b***

Yield 67–69%, m.p. 123–125°C. White powder. ^{1}H NMR spectrum: 4.30 (s, 2H, CH$_2$, *J* 14.3), 6.96 (s, 2H, NH$_2$), 11.24 (br.s., 1H, COOH); 12.61 (s, 1H, NH). Found, *m/z*: 191.0229 [M+H]$^+$. C$_4$H$_6$N$_4$O$_3$S+H$^+$. Calculated, *m/z*: 191.0234 [M+H]$^+$.

2.3. Electrochemical studies

Electrochemical measurements were carried out in a borate buffer solution in the presence of an activating additive of 0.01 mol/L NaCl. Studies in this solution provide information on the passivating action of triazoles and their ability to stabilize the passive state of copper under conditions of competitive adsorption of organic inhibitor and chloride.

Full cathodic and anodic potentiodynamic polarization curves were recorded. Polarization curves were obtained on copper electrodes (area 0.75 cm^2, designated as M1) in an undivided electrochemical cell using an IPC-PRO potentiostat. The working electrode was pre-cleaned with K2000 sandpaper and degreased with ethanol. Electrode potentials (*E*) were measured relative to a silver chloride electrode, connected through an electrolytic bridge based on agar-agar and sodium nitrate, and converted to the scale of a standard hydrogen electrode (potential +201 mV *vs.* SHE). The auxiliary electrode was a platinum mesh.

After the formation of the copper oxide film in air, at *E*=−0.60 V for 15 minutes, polarization was discontinued until the open circuit potential (*E*$_{corr}$) stabilized. The time to reach a steady state was 3 to 5 minutes. Then, with stirring, NaCl solution (concentration C_{Cl^-}=0.01 mol/L) and the studied inhibitors were introduced. After stabilizing the new *E*$_{corr}$ value for 3–5 minutes, polarization curves were recorded with a potential scan rate of 0.2 mV/s. The activation potential (*E*$_{pitt}$) was determined by the sharp increase in current on the polarization curve, followed by visual identification of pitting corrosion on the electrode surface. The uncertainty in *E*$_{pitt}$ measurement was ±0.05 V.

Measurements for each substance concentration were performed at least 5 times to obtain reproducible data, followed by statistical analysis of the measurement results.

2.4. Direct corrosion tests

The tests were conducted in accordance with GOST 9.905-82 "Methods of corrosion testing" and GOST 9.907-83 "Methods of removing products after corrosion testing".

Sample preparation

Corrosion tests were conducted on copper plates (20×50 mm, thickness 0.2 mm). Each sample was pre-polished with fine-grained sandpaper K2000, then rinsed with distilled water, ethanol, and dried with filter paper. The experiments were carried out in a 1% HCl solution (for 7 days) under natural aeration without stirring for three samples simultaneously (for each inhibitor concentration, as in the tables). After the tests, the plates were rinsed with distilled water and treated with compositions according to GOST 9.907-83.

The corrosion rate was determined based on the mass loss of the samples and calculated using the formula:

$$k_{inh} = \frac{m_0 - m}{S \cdot t},$$

where $\Delta m = m_0 - m$ (m_0 is the mass of the sample before the experiment, m is the mass of the sample after the test in grams); S is the area of the plate in square meters.

The inhibiting efficiency of the aminotriazole derivatives was evaluated based on the inhibition efficiency coefficient $\gamma = k_0/k_{inh}$ and the degree of protection

$$Z_k = \frac{(k_0 - k_{inh})}{k_0} \cdot 100\% ,$$

where k_0 and k_{inh} are the corrosion rates in the HCl solution without inhibitor and with inhibitor, respectively. The value of the k_0 parameter was ~22.8 g·m^{-2}·day^{-1}.

The investigation of anti-corrosion activity was conducted for systems with inhibitor concentrations of 10 mM, 5 mM, and 1 mM.

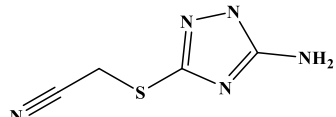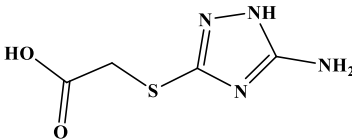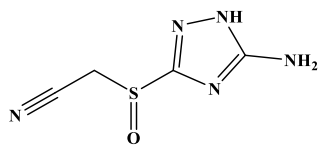*Testing methodology in a salt spray chamber*

Atmospheric corrosion of copper was accelerated using the salt spray test to assess the effectiveness of studied inhibitors for interoperative protection of copper products. Protective inhibitor films were obtained by exposing copper plates to an inhibitor-containing aqueous solution for 60 minutes at 60°C. Samples were wiped with filter paper and air-dried at room temperature for 2 hours, then placed in a sealed chamber with a volume of 14,000 cm^3 and 95–100% air humidity. A 5% NaCl (pH 6.5–7.2, according to GOST R 52763-2007) solution was sprayed in the chamber using a pump with 6 hydraulic nozzles, automatically activated for 1 second every hour (solution flow rate per nozzle ~7 mL). Samples were examined three times a day to determine the time of first signs of corrosion (τ_{corr}).
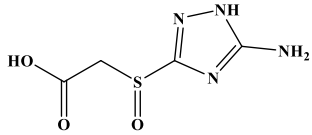
3. Results and Discussion

The results of the direct corrosion tests of the investigated inhibitors are presented in Table 2. The tests in a 1% HCl solution revealed that the 5-amino-1,2,3-triazoles **2a** and **3a**, containing thioacetonitrile and sulfinylacetonitrile fragments, exhibited the highest

efficiency. The introduction of the acetic acid fragment into the structure of 5-amino-1,2,3-triazole (inhibitors **2b**, **3b**) negatively affected their protective properties. This pattern is most likely related to the corrosion inhibition mechanism of this class of compounds, which has been extensively described in previous publications. This mechanism can be characterized by the "head-tail" principle, which involves the formation of an adsorbed layer of the 1,2,4-triazole derivative, complexed with copper atoms in the studied chloride-containing media. The triazole matrix acts as the "head", ensuring the adsorption of the molecule on the metal surface through the aforementioned complexation mechanism via N–H acidity, along with additional coordination, hydrogen bonding, Van der Waals, and other types of binding. Electron-accepting substituents in the 3rd position of the triazole can increase the tendency for complexation by enhancing the N–H acidity of the endo-nitrogen atom, following the ligand-acceptor principle. Meanwhile, the side chain, specifically the substituents in the 3rd position of the triazole ring, serves as the "tail", providing sufficient hydrophobicity and limiting the contact of the aggressive medium with the metal surface, thus ensuring the protective properties of the inhibitor. We hypothesize that for the 5-amino-1,2,3-triazoles **2a** and **3a** with thioacetonitrile and sulfinylacetonitrile substituents, the primary factor determining the overall inhibitor efficiency is the high electron-accepting effect of these substituents while maintaining their hydrophobicity. In the case of acetic acid derivatives **2b** and **3b**, the carboxyl fragment, on the contrary, exhibits higher hydrophilicity and promotes greater interaction with the medium, reducing the degree of inhibitor film adsorption on the surface and consequently lowering the protection efficiency.

Table 2. Results of determining the corrosion rates k, inhibition coefficients γ, protection degrees Z, and the time of the first signs of corrosion in the salt spray chamber τ based on the direct corrosion tests.

Inhibitor	C_{inh}, mol/L	k, g·m^{-2}·day^{-1}	γ	Z, %	τ, hour
without	0	~22.8	–	–	2
2a	10	11.0	2.1	51.75	44
	5	6.9	3.3	69.74	41
	1	13.3	1.7	41.67	39
2b	10	21.6	1.1	5.26	28
	5	21.9	1.0	3.95	25
	1	22.6	1.0	0.88	20
3a	10	2.3	9.9	89.91	40
	5	2.8	8.1	87.72	37
	1	7.6	3.0	66.67	28

Inhibitor	C_{inh}, mol/L	k, g·m^{-2}·day^{-1}	γ	Z, %	τ, hour
(structure)	10	13.7	1.7	39.91	30
	5	15.9	1.4	30.26	22
3b	1	15.3	1.5	32.89	19

Polarization curves obtained on copper in solutions with the addition of the investigated compounds are shown in Figure 1.
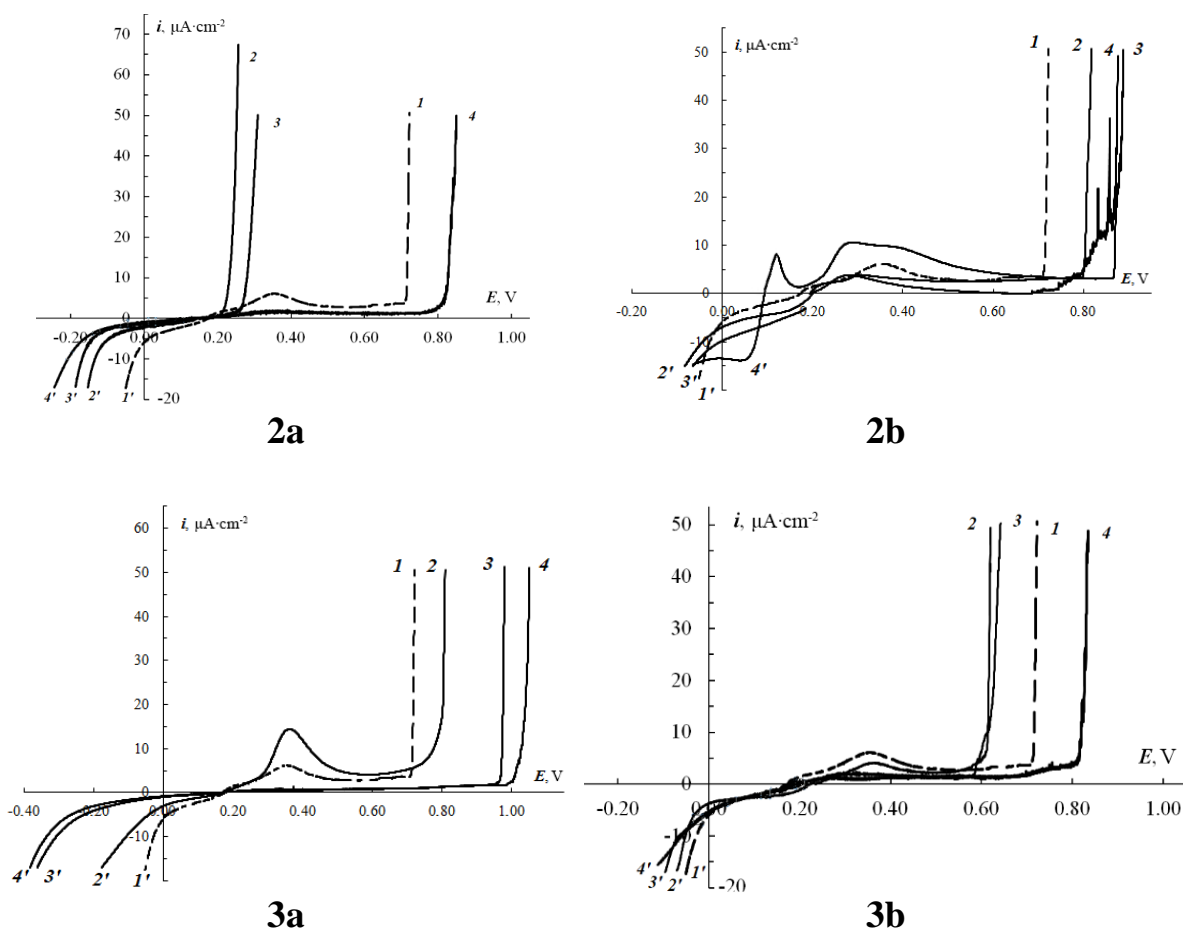

Figure 1. Anodic (*1–4*) and cathodic (*1'–4'*) polarization curves obtained on copper in borate buffer (pH=7.40) with the addition of 0.01 M NaCl and 3-(sulfinyl(5-amino-1*H*-1,2,4-triazol-1-yl) acetic acid with concentration C_{inh} (mmol·dm^{-3}): *1, 1'* – without addition; *2, 2'* – 0.01; *3, 3'* – 0.10; *4, 4'* – 1.00.

When adding 2-((5-amino-1*H*-1,2,4-triazol-3-yl)mercapto)acetonitrile **2a** in concentrations of 0.01, 0.10, and 1.00 mmol·dm^{-3}, E_{corr} shifts to the cathodic region by ~15 mV, ~25 mV, and ~55 mV relative to the control experiment, respectively. At the initial sections of the anodic polarization curves, a decrease in current density relative to the control

experiment was observed for all studied concentrations. For additive concentrations of 0.01 and 0.10 mmol·dm^{-3}, the shift of the potential by ~+40 mV and ~+125 mV relative to E_{corr} on the anodic polarization curve is accompanied by an increase in anodic current density, with no passivation region present. At an additive concentration of 1.00 mmol·dm^{-3}, the active dissolution peak of copper does not form, and the anodic current density remains constant up to pitting potentials E_{pitt} of ~+0.81 V. At E_{pitt}, the anodic current increases sharply, and the potential itself is shifted by approximately +90 mV relative to the control experiment. The passivation current density is up to two times lower compared to the control experiment.

For the cathodic polarization curves, an expansion of the low cathodic current region (the polarization curve is pressed to the zero current axis) is noted. The position of the region of increasing cathodic current density is shifted by ~−100 to −250 mV relative to the control experiment. Protective action of mercaptopropyl-1H-1,2,4-triazole can be assumed at a concentration of no less than 1 mmol·dm^{-3}.

Table 3. Results of E_{corr} control and calculation of corrosion current i_{corr} for solutions containing 2-((5-amino-1H-1,2,4-triazol-3-yl)sulfinyl)acetic acid.

Inhibitor	E_{corr}, mV			
C_{inh}	–	0.01	0.10	1.00
2a	+176	+160	+150	+120
2b	+176	+200	+200	+75
3a	+176	+174	+179	+200
3b	+176	+230	+210	+179

Upon the introduction of 3-[mercapto-(5-amino-1H-1,2,4-triazole)-1-yl]-acetic acid **2b** at concentrations of 0.01 mmol/L and 0.10 mmol/L, E_{corr} shifts to the anodic region by approximately 25 mV relative to the control experiment. At an additive concentration of 1.00 mmol/L, the open-circuit potential, E_{corr}, shifts to the cathodic region by approximately 100 mV relative to the control experiment. In the initial sections of the anodic polarization curves for additive concentrations of 0.01 mmol/L and 0.10 mmol/L, an increase in current density is observed up to potentials of approximately +260 mV and +300 mV, respectively, which is close to the control experiment. The position of the anodic current density maxima is lower than in the control experiment and is shifted cathodically by 100 mV and 50 mV, respectively, along the potential axis. After passing the maximum, the current decreases and remains constant up to E_{pitt} values of approximately +800 mV and +900 mV, respectively. Activation occurs, accompanied by a sharp increase in anodic current density. The passivation current density is similar to that of the control experiment for the additive concentration of 0.01 mmol/L and is twice as low for the additive concentration of

0.10 mmol/L. The value of E_{pitt} is 100–150 mV more positive relative to the control experiment.

For a concentration of 3-[mercapto-(5-amino-1*H*-1,2,4-triazole)-1-yl]-acetic acid at 1.00 mmol/L, the polarization curve has a more complex appearance. The initial section is accompanied by an intense increase in current density, forming two current density maxima. The position of the anodic current density maxima along the potential axis is more negative by approximately 200 mV relative to the control experiment. During further polarization, the current decreases to a E of approximately +160 mV, after which it increases again. The second peak forms at a potential of +300 mV. For the maxima, the current density exceeds the control value by 1.5–2.0 times. During further polarization, the current density decreases smoothly to values close to the control experiment up to the E_{pitt} of approximately +900 mV, where a sharp increase in anodic current density is observed. The value of E_{pitt} is 200 mV more positive relative to the control experiment.

The cathodic polarization curves obtained on copper for 3-[mercapto-(5-amino-1*H*-1,2,4-triazole)-1-yl]-acetic acid at concentrations of 0.01 mmol/L and 0.10 mmol/L are close to the control polarization curve. For an additive concentration of 1.00 mmol/L, a sharp increase in cathodic current density is observed in the initial stage. Thus, 3-[mercapto-(5-amino-1*H*-1,2,4-triazole)-1-yl]-acetic acid does not provide a protective effect at the investigated concentrations.

Upon the introduction of 2-((5-amino-1*H*-1,2,4-triazole-3-yl)sulfinyl)acetonitrile **3a** up to 0.10 mmol·dm^{-3}, E_{corr} is similar to the value of the control experiment. At an additive concentration of 1.00 mmol·dm^{-3}, a shift of E_{corr} to the anodic region by approximately 25 mV relative to the control experiment is observed. In the initial sections of the anodic polarization curves, a decrease in current density relative to the control experiment is observed up to a E of approximately +250 mV for all studied concentrations. For an additive concentration of up to 0.01 mmol·dm^{-3}, with further polarization, an increase in anodic current density is observed, which exceeds the control value by more than 2 times at the maximum point. The position of the anodic current density maximum along the potential axis is close to the control experiment at approximately +380 mV. After passing the maximum, the current decreases and remains constant up to the E_{pitt} of approximately +750 mV, where a sharp increase in current density is observed, *i.e.*, the value of E_{pitt} is approximately 100 mV more positive relative to the control experiment. The passivation current density is similar to the control experiment within the measurement error. For an additive concentration of 0.10 mmol·dm^{-3} of 2-((5-amino-1*H*-1,2,4-triazole-3-yl)sulfinyl)acetonitrile **3a**, a maximum current does not form, and the current density remains constant up to the activation potential (approximately +950 mV) – a shift relative to the control by approximately +300 mV. The current density in the passivity region can be up to three times lower than in the control experiment. Upon the introduction of an additive concentration of 1.00 mmol·dm^{-3}, a maximum current also does not form. The further course of the anodic polarization curve is similar to the experiment with the additive of 0.10 mmol·dm^{-3}. E_{pitt} is shifted relative to the control by approximately +400 mV.

Cathodic polarization curve at a concentration of 2-((5-amino-1*H*-1,2,4-triazole-3-yl)sulfinyl)acetonitrile **3a** 0.01 mmol·dm^{-3} shows an expansion of the region of small cathodic currents (the curves are pressed to the zero current axis) by 30–40 mV. When the additive is introduced at 0.10 mmol·dm^{-3} and higher, the position of the rising cathodic current density region shifts by 180–200 mV relative to the control experiment.

Comparison of the results of the anodic and cathodic polarization curves and the calculation of the corrosion current density suggests the protective effect of 2-((5-amino-1*H*-1,2,4-triazole-3-yl)sulfinyl)acetonitrile **3a** at concentrations of 0.10 mmol·dm^{-3} and higher. A protective effect of at least three times is noted.

At the minimum studied concentration of 2-((5-amino-1*H*-1,2,4-triazole-3-yl)sulfinyl)acetic acid **3b** (0.01 mmol·dm^{-3}), E_{corr} shifts to the anodic region by approximately 55 mV relative to the control experiment. At an additive concentration of 0.10 mmol·dm^{-3}, E_{corr} shifts to the anodic region by approximately 35 mV. At an additive concentration of 1.00 mmol·dm^{-3}, the open-circuit potential is similar to the control experiment. In the initial sections of the anodic polarization curves, a decrease in current density is noted relative to the control experiment up to a potential of approximately +230 mV for all studied concentrations. At an additive concentration of 0.01 mmol·dm^{-3}, with further polarization, the anodic current density increases, which is half the control value at the maximum point. The position of the maximum anodic current density on the potential axis is close to that in the control experiment, $E \sim +350$ mV. After passing the maximum, the current decreases and remains constant up to the E_{pitt} of approximately +600 mV. Activation is accompanied by a sharp increase in anodic current density. The passivation current density is close to the control experiment. The electrode potential, at which the anodic current sharply increases, is approximately 130 mV more negative relative to the control experiment. At an additive concentration of 0.10 mmol·dm^{-3}, the current maximum on the anodic polarization curve does not form. The passivation current density is twice as low as the control experiment. E_{pitt} is shifted by approximately –130 mV relative to the control. When the additive is introduced at 1.00 mmol·dm^{-3}, the current maximum does not form. The further course of the anodic polarization curve is similar to the experiment with the additive of 0.10 mmol·dm^{-3}. E_{pitt} shifts by +100 mV relative to the control.

Cathodic polarization curves obtained on copper for all concentrations of 2-((5-amino-1*H*-1,2,4-triazole-3-yl)sulfinyl)acetic acid are hardly distinguishable from the control curve within the measurement error. Comparison of the results of the anodic and cathodic polarization curves suggests the protective effect of 2-((5-amino-1*H*-1,2,4-triazole-3-yl)sulfinyl)acetic acid at concentrations of about 1.00 mmol·dm^{-3}. In this case, the protective effect may be no more than 1.5–2 times.

For inhibitor **3a**, which exhibited the best protective characteristics in both direct and electrochemical tests, studies of the adsorption layer formed on the copper surface were conducted using scanning electron microscopy combined with surface elemental analysis. According to the surface elemental analysis (Table 4), it is evident that after exposure to the inhibitor **3a** solution, there is deposition of the inhibitor on the surface (nitrogen and sulfur

content of 6.46% and 3.44%, respectively). In the case of exposure to the inhibitor solution in 1% HCl, the sulfur, nitrogen, and chlorine content increases even more significantly. These results indicate the formation of an inhibitor complex film on the copper surface, formed with the participation of dissolved copper ions and chloride ions.

Table 4. Elemental surface composition (at. %) of the copper electrode.

Plate	Cu, at. %	N, at. %	S, at. %	Cl, at. %
(a)	96.36	3.64	–	–
(b)	90.10	6.46	3.44	–
(c)	77.11	–	–	22.89
(d)	71.21	12.90	6.78	9.11

In the provided images (Figure 2), it is evident that the surface of the plate (c) is severely damaged due to corrosion, showing significant dissolution and oxidation of the copper layer – the surface is porous, with substantial pits and irregularities. Meanwhile, the copper sample (d) that was exposed to a 1% HCl solution in the presence of 10 mmol/l of inhibitor **3a** retained the overall surface structure, with no significant pitting observed. Even to the naked eye, it is visible that a glass-like layer has formed on the plate, most likely a self-organized film of the complex based on the inhibitor and dissolved copper ions. This effect can also be observed in the micrographs in Figure 2 (d) – the investigated surface is almost entirely smooth, with the scratches from the sandpaper greatly diminished compared to the copper before the corrosion tests.

The fact that such an effect is observed only in the case of the plate after exposure to 1% HCl solution with the inhibitor, as well as the results of elemental analysis, indicate that the formation of complexes with copper atoms and chloride ions presumably occurs in the structure shown below.
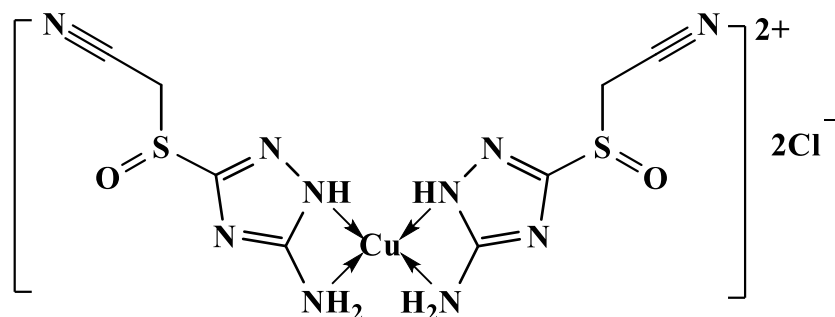
Thus, the studied derivatives of aminotriazoles with thioacetonitrile and sulfinylacetonitrile substituents can be considered promising copper corrosion inhibitors under chloride corrosion conditions at concentrations from 0.10 mmol/dm^3.
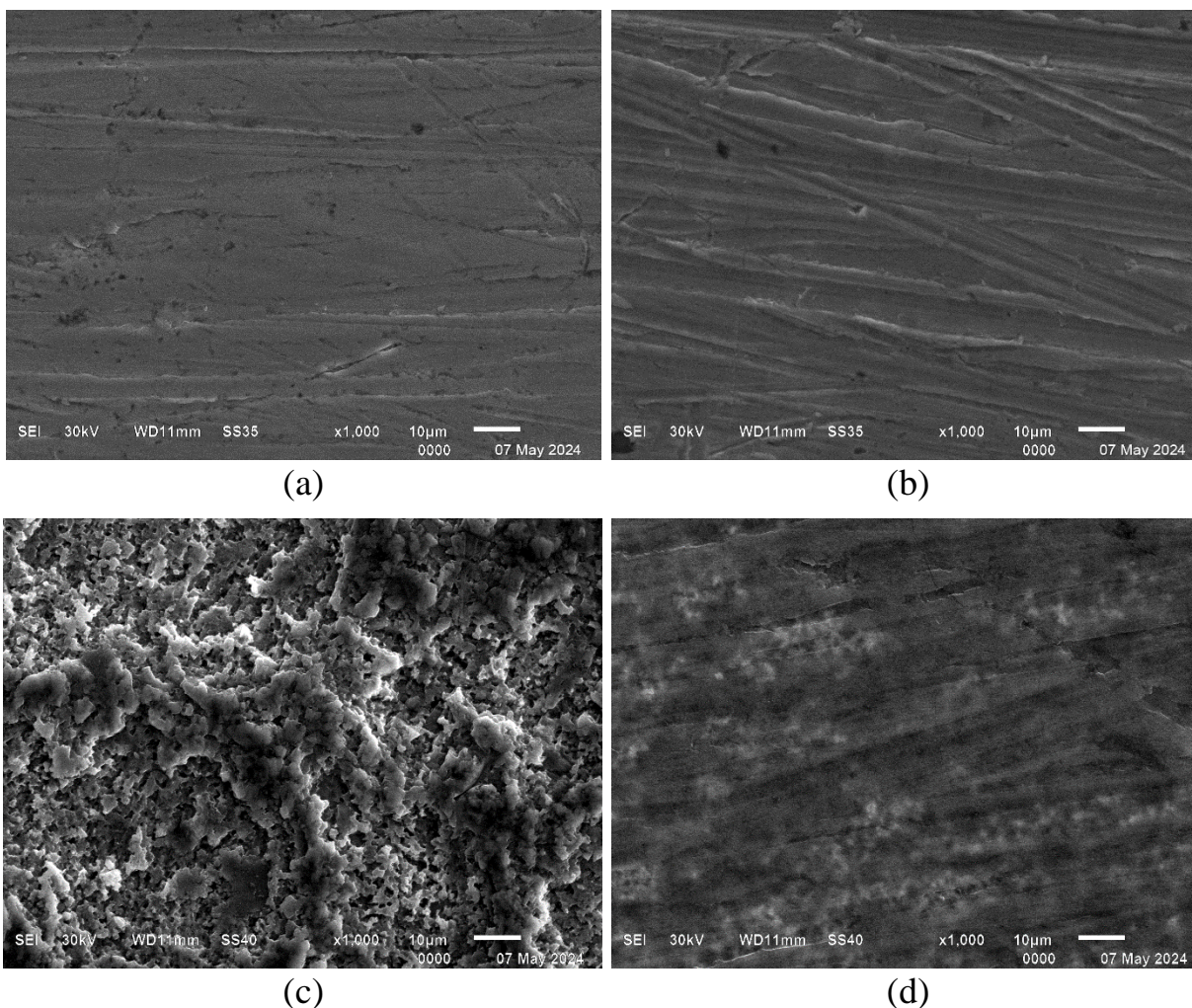
Figure 2. SEM micrographs of the copper surface (a) before corrosion tests in 1% HCl, (b) before corrosion tests in 1% HCl+10 mmol/l inhibitor **3a**, (c) after corrosion tests in 1% HCl, and (d) after corrosion tests in 1% HCl+10 mmol/l inhibitor **3a**.

Conclusion

This study confirms the high potential of 5-amino-1*H*-1,2,4-triazole derivatives, particularly those containing thioacetonnitrile and sulfinylacetonitrile fragments, as effective inhibitors of copper corrosion in chloride environments. Among the substances studied, 2-((5-amino-1*H*-1,2,4-triazol-3-yl)sulfinyl)acetonitrile **3a**, at a very low concentration of 0.10 mmol·dm^{-3}, demonstrated good anticorrosion properties with $Z=87\%$ according to corrosion tests. These results are consistent with studies using the potentiodynamic polarization method. Anodic polarization curves obtained upon their addition showed a significant shift in the E_{pitt}, indicating a high degree of anodic passivation on copper in the presence of the investigated compounds. On the other hand, analysis of cathodic curves revealed that all studied compounds shift the region of cathodic current increase towards the cathodic area by 180–200 mV. Thus, the obtained direct and potentiodynamic experimental results correlate well with each other. Results from SEM analysis indicate the formation of a complex compound

film on the metal surface based on copper, 2-((5-amino-1*H*-1,2,4-triazol-3-yl)sulfinyl)-acetonitrile **3a**, and chloride ions.

Therefore, it is demonstrated that introducing a sulfinylacetonitrile substituent at the third position of the 5-amino-1*H*-1,2,4-triazole molecule has a positive influence on the anti-corrosive properties of such an inhibitor regarding copper corrosion in 1% chloride-containing solutions.

Acknowledgments

References

1. M.O. Isei, D. Stevens and C. Kamunde, Temperature rise and copper exposure reduce heart mitochondrial reactive oxygen species scavenging capacity, *Comp. Biochem. Physiol.*, *Part C: Toxicol. Pharmacol.*, 2021, **243**, 108999. doi: 10.1016/j.cbpc.2021.108999

2. Ž.Z. Tasić, M.B. Petrović Mihajlović, M.B. Radovanović and M.M. Antonijević, New trends in corrosion protection of copper, *Chem. Pap.*, 2019, **73**, 2103–2132. doi: 10.1007/s11696-019-00774-1

3. G. Kear, B.D. Barker and F.C. Walsh, Electrochemical corrosion of unalloyed copper in chloride media – a critical review, *Corros. Sci.*, 2004, **46**, no. 1, 109–135. doi: 10.1016/s0010-938x(02)00257-3

4. M. Finsgar and I. Milosev, Inhibition of copper corrosion by 1,2,3-benzotriazole: A review, *Corros. Sci.*, 2010, **52**, no. 9, 2737–2749. doi: 10.1016/j.corsci.2010.05.002

5. D.S. Chauhan, M.A. Quraishi, W.B. Wan Nik and V. Srivastava, Triazines as a potential class of corrosion inhibitors: Present scenario, challenges and future perspectives, *J. Mol. Liq.*, 2021, **321**, 114747. doi: 10.1016/j.molliq.2020.114747

6. E. Kabir and M. Uzzaman, A review on biological and medicinal impact of heterocyclic compounds, *Results Chem.*, 2022, **4**, 100606. doi: 10.1016/j.rechem.2022.100606

7. Yu.I. Kuznetsov and L.P. Kazanskiy, Physicochemical aspects of metal protection by azoles as corrosion inhibitors, *Russ. Chem. Rev.*, 2008, **77**, no. 3, 219–232. doi: 10.1070/RC2008v077n03ABEH003753

8. Yu.I. Kuznetsov, Triazoles as a class of multifunctional corrosion inhibitors. Review. Part V. 1*H*-1,2,4-triazole and its derivatives. Copper and its alloys, *Int. J. Corros. Scale Inhib.*, 2022, **11**, no. 3, 965–979. doi: 10.17675/2305-6894-2022-11-3-5

9. J. Schapira, J. Vincent and L.R. Lovy Aime, New application of aminotriazole, composition containing it. and process for its use, *FR Patent*, 2656630, C23F11, 1991.

10. Yu.I. Kuznetsov, Y.G. Avdeev and O.O. Zel, Inhibitor of acid metal corrosion, *RU Patent*, 2539129, C23F11/04, 2015.

11. Yu.I. Kuznetsov, L.V. Frolova, Y.G. Avdeev, N.N. Andreev and O.O. Zel, Inhibitor of sulphide corrosion and hydrogenation of metal hardware, *RU Patent*, 2539132, C23F11/04, 2015.

12. Yu.B. Makarychev, I.A. Arkhipushkin, T.A. Karpukhina, Kh.S. Shikhaliev and L.P. Kazanskiy, Formation of nanolayers by some azoles on the surface from aqueous solutions. Pt. 1, *Korroz.: Mater., Zashch. (Corrosion: Materials, Protection)*, 2016, no. 2, 20–27 (in Russian).

13. Z. Khiati, A.A. Othman, M. Sanchez-Moreno, M.C. Bernard, S. Joiret, E.M.M. Sutter and V. Vivier, Corrosion inhibition of copper in neutral chloride media by a novel derivative of 1,2,4-triazole, *Corros. Sci.*, 2011, **53**, no. 10, 3092–3099. doi: 10.1016/j.corsci.2011.05.042

14. M. Finšgar, EQCM and XPS analysis of 1,2,4-triazole and 3-amino-1,2,4-triazole as copper corrosion inhibitors in chloride solution, *Corros. Sci.*, 2013, **77**, 350–359. doi: 10.1016/j.corsci.2013.08.026

15. E.A. Skrypnikova, S.A. Kaluzhina and L.E. Agafonova, Inhibition of copper pitting corrosion in alkaline sulphate media by benzotriazole at elevated temperatures, *lnt. J. Corros. Scale Inhib.*, 2014, **3**, no. 1, 59–65. doi: 10.17675/2305-6894-2014-3-1-059-065

16. I. Dugdale and J.B. Cotton, An electrochemical investigation on the prevention of staining of copper by benzotriazole, *Corros. Sci.*, 1963, **3**, no. 2, 69–75. doi: 10.1016/s0010-938x(63)80001-3

17. G.W. Poling, Reflection infra-red studies of films formed by benzotriazole on Cu, *Corros. Sci.*, 1970, **10**, no. 5, 359–370. doi: 10.1016/s0010-938x(70)80026-9

18. O.A. Goncharova, A.Yu. Luchkin, N.N. Andreev, N.P. Andreeva and S.S. Vesely, Triazole derivatives as chamber inhibitors of copper corrosion, *Int. J. Corros. Scale Inhib.*, 2018, **7**, no. 4, 657–672. doi: 10.17675/2305-6894-2018-7-4-12

19. Yu.I. Kuznetsov, New possibilities of metal corrosion inhibition by organic heterocyclic compounds, *Int. J. Corros. Scale Inhib.*, 2012, **1**, no. 1, 3–15. doi: 10.17675/2305-6894-2012-1-1-003-015

20. Yu.I. Kuznetsov and L.P. Podgornova, Inhibition of metal corrosion by heterocyclic chelating reagents, *Itogi Nauki i Tekhiki, Ser.: Korroz. Zashch. Korroz. (Advances in Science and Technology, Ser.: Corrosion and Corrosion Protection)*, Moscow, VINITI, 1989, vol. 15, 132–185 (in Russian).

21. K. Es-Salah, M. Keddam, K. Rahmouni, A. Srhiri and H. Takenouti, Aminotriazole as corrosion inhibitor of Cu-30Ni alloy in 3% NaCl in presence of ammoniac, *Electrochim. Acta*, 2004, **49**, no. 17–18, 2771–2778. doi: 10.1016/j.electacta.2004.01.038

22. M.N.H. Moussa, A.A. El-Far and A.A. El-Shafei, The use of water-soluble hydrazones as inhibitors for the corrosion of C-steel in acidic medium, *Mater. Chem. Phys.*, 2007, **105**, no. 1, 105–113. doi: 10.1016/j.matchemphys.2007.04.007

23. L.M. Rivera-Grau, M. Casales, I. Regla, D.M. Ortega Toledo, J.A. Ascencio-Gutierrez, J.P. Calderon and L. Martinez-Gomez, Effect of organic corrosion inhibitors on the

corrosion performance of 1018 carbon steel in 3% NaCl solution, *Int. J. Electrochem. Sci.*, 2013, **8**, 2491–2503.

24. D.S. Shevtsov, Kh.S. Shikhaliev, N.V. Stolpovskaya, A.A. Kruzhilin, A.Yu. Potapov, I.D. Zartsyn, O.A. Kozaderov, D.V. Lyapun, C. Prabhakar and A. Tripathi, 3-Alkyl-5-amino-1,2,4-triazoles synthesized from the fatty acids of sunflower oil processing waste as corrosion inhibitors for copper in chloride environments, *Int. J. Corros. Scale Inhib.*, 2020, **9**, no. 2, 726–744. doi: 10.17675/2305-6894-2020-9-2-21

25. O.A. Kozaderov, Kh.S. Shikhaliev, Ch. Prabhakar, A. Tripathi, D.S. Shevtsov, A.A. Kruzhilin, E.S. Komarova, A.Yu. Potapov, I.D. Zartsyn and Yu.I. Kuznetsov, Corrosion of α-Brass in Solutions Containing Chloride Ions and 3-Mercaptoalkyl-5-amino-1H-1,2,4-triazoles, *Appl. Sci.*, 2019, **9**, no. 14, 2821. doi: 10.3390/app9142821

26. O.A. Kozaderov, Kh.S. Shikhaliev, C. Prabhakar, D.S. Shevtsov, A.A. Kruzhilin, E.S. Komarova, A.Yu. Potapov and I.D. Zartsyn, Copper corrosion inhibition in chloride environments by 3-(*N*-hetaryl)-5-amino-1*H*-1,2,4-triazoles, *Int. J. Corros. Scale Inhib.*, 2019, **8**, no. 2, 422–436. doi: 10.17675/2305-6894-2019-8-2-19

27. A.A. Kruzhilin, D.V. Lyapun, D.S. Shevtsov, O.A. Kozaderov, A.Yu. Potapov, I.D. Zartsyn, Ch. Prabhakar and Kh.S. Shikhaliev, New [1,2,4]triazolo[1,5-*a*] pyrimidine-7-one corrosion inhibitors for copper in chloride environments, *Int. J. Corros. Scale Inhib.*, 2021, **10**. no. 4, 1474–1492. doi: 10.17675/2305-6894-2021-10-4-7

28. A.A. Kruzhilin, D.S. Shevtsov, D.V. Lyapun, A.Yu. Potapov, O.A. Kozaderov, E.V. Nikitina and Kh.S. Shikhaliev, Bis-[(5-amino-1*H*-1,2,4-triazol-3-yl)mercapto]alkanes – novel twin compounds as copper corrosion inhibitors in high chloride containing media, *Int. J. Corros. Scale Inhib.*, 2023, **10**, no. 1, 244–257. doi: 10.17675/2305-6894-2023-12-1-14

29. N.W. Liu, S. Liang and G. Manolikakes, Recent Advances in the Synthesis of Sulfones, *Synthesis*, 2016, **48**, no. 13, 1939–1973. doi: 10.1055/s-0035-1560444

30. M.J. Frisch, G.W. Trucks, H.B. Schlegel, G.E. Scuseria, M.A. Robb, J.R. Cheeseman, G. Scalmani, V. Barone, G.A. Petersson, H. Nakatsuji, X. Li, M. Caricato, A.V. Marenich, J. Bloino, B.G. Janesko, R. Gomperts, B. Mennucci, H.P. Hratchian, J.V. Ortiz, A.F. Izmaylov, J.L. Sonnenberg, D. Williams-Young, F. Ding, F. Lipparini, F. Egidi, J. Goings, B. Peng, A. Petrone, T. Henderson, D. Ranasinghe, V.G. Zakrzewski, J. Gao, N. Rega, G. Zheng, W. Liang, M. Hada, M. Ehara, K. Toyota, R. Fukuda, J. Hasegawa, M. Ishida, T. Nakajima, Y. Honda, O. Kitao, H. Nakai, T. Vreven, K. Throssell, J.A. Montgomery, Jr., J.E. Peralta, F. Ogliaro, M.J. Bearpark, J.J. Heyd, E.N. Brothers, K.N. Kudin, V.N. Staroverov, T.A. Keith, R. Kobayashi, J. Normand, K. Raghavachari, A.P. Rendell, J.C. Burant, S.S. Iyengar, J. Tomasi, M. Cossi, J.M. Millam, M. Klene, C. Adamo, R. Cammi, J.W. Ochterski, R.L. Martin, K. Morokuma, O. Farkas, J.B. Foresman and D.J. Fox, *Gaussian 16, Revision B.01*, Gaussian, Inc., Wallingford CT, 2016.

31. R.G. Parr and R.G. Pearson. Absolute hardness: companion parameter to absolute electronegativity, *J. Am. Chem. Soc*., 1983, **105**, no. 26, 7512–7516. doi: 10.1021/ja00364a005

♦ ♦ ♦